Proceedings of the 2007 IEEE/RSJ International Conference on Intelligent Robots and Systems
San Diego, CA, USA, Oct 29 - Nov 2, 2007

Roughness Feeling Telepresence System on the Basis of Real-time Estimation of Surface Wavelengths

Shogo Okamoto, Masashi Konyo, Takashi Maeno and Satoshi Tadokoro

Abstract— **Tactile telepresence has been expected to be technology which encourages operators of robotic systems to remotely maneuver objects or recognize materials being touched through robotic arms. In remote environments, temporal disparity in tactile sensations is caused by temporal latency between a touch motion of the operator and a tactile stimulus applied on him. A framework of tactile telepresence systems, which is suitable in remote environments, has been proposed in the present paper. In the framework, a tactile display locally generates the tactile stimulus in synchronization with the touch motion of the operator in order to cancel communication delay. The tactile stimulus is generated by combining the motion and tactile factors, which are sensed by a tactile sensor. The factors are characteristic parameters of objects and effect on tactile sensations. In the present paper, physical parameters of the objects are selected as the factors because the tactile stimuli can be computed using physical models involving the motions and the parameters. Based on the proposed framework, a roughness feeling telepresence system was implemented and successfully transferred a roughness factor to the operator.**

I. INTRODUCTION

Tactile telepresence technology, which enables operators of robotic systems to feel sense of touch like roughness or softness feelings, has been expected to promote robotic solutions in various fields. For instance, tactile information processing would allow operators of remote manipulation systems to detect incipient slippage on holding objects or to recognize materials of objects. The final aim of the present project is transferring to operators realistic tactile sensations which are acquired by robots in remote environments.

In general, a tactile telepresence system is composed of tactile sensors which sense tactile information instead of human operators, tactile displays which artificially synthesize cutaneous sensations, and a master-slave robotic system which connects the sensors and the displays.

As related works, palpation systems for minimally invasive surgery [1][2]!$the systems which transferred softness feelings [3] and texture sensations [4] were reported. These related works can be classified into the same group from the point of view of information communication from the tactile sensor systems to display systems. In these systems, tactile sensors detected physical phenomena which occured at the sensor side, such as deformation of the sensor or states of contacts. Tactile information sensed by the tactile sensors was sequentially transferred to the display side systems through networks. Then tactile displays reproduced similar physical phenomena on the fingers of operators.

These existing technology has not considered active touch in remote environments. Even if the existing methods were applied to tactile telepresence in remote environments, latency between a touch motion of the operator and tactile feedback would complicate active touch. Latency causes temporal disparity in tactile sensations. For instance, if an operator could not sense any tactile feedback when he started his motions, subjective wrongness would occur in his sensations. Wrongness is caused by a mismatch between the motion and the tactile stimulus.

This study has proposed a new framework which is suitable in remote environments and solves the above problem. In the framework, stimuli generation by a local loop in the display side system cancels sensory mismatches between kinetic and tactile sensations. Because the local loop recomputes the tactile stimuli based on the motions of the operator and tactile factors which are sensed and transferred by the sensor. The tactile factor is any information, from which the stimuli can be computed by combining with the motions in the display side system. In this study, the tactile factors are physical parameters of objects since generally physical relationships between the physical parameters, the motions and the stimuli can be utilized.

In implementing the framework, it is preferable that physical parameters of target objects are estimated in real-time. Because once physical parameters are estimated and transferred to the display system, then the display can produce tactile stimuli without latency between the hand movements of an operator, however, until they are transferred proper stimuli cannot be generated. The framework cannot resolve problems of communication time-delay themselves; however temporal disparity in tactile sensations due to latency can be canceled. The framework is considered to be effective when materials of the object are not frequently varying.

A prototype of a roughness feeling telepresence systems has been developed following the proposed framework. According to early psychophysical studies, the relationships between physical parameters and roughness sensations are clearer than other tactile sensations, which helps the discussion to concentrate on the effectiveness of the proposed framework. However, the proposed framework can be applied to other tactile sensations like softness, moistness and thermal feelings.

S. Okamoto, M. Konyo and S. Tadokoro are with Graduate School of Information Sciences, Tohoku University, 6-6-01, Aramaki Aza Aoba, Aoba-ku, Sendai, 980-8579, Japan {okamoto, konyo, tadokoro}@rm.is.tohoku.ac,jp

T. Maeno is with Department of Science and Technology, Keio University, 3-14-1 Hiyoshi, Kohoku-ku, Yokohama, 223-8522, Japan maeno@mech.keio.ac.jp

II. Design of Roughness Feelings Telepresence System Based on Real-time Estimation of Surface Wavelengths

A framework for the proposed tactile telepresence system in remote environments is described in this section.

In the framework, a hand of an operator and a robotic arm are connected by a master-slave system so that the system achieves tactile sensing according to his hand movements. The human hand is equipped with a tactile display, and a tactile sensor is installed on a tip of the robotic arm. As the human hand moves, the robotic arm moves and the tactile sensor estimates physical parameters of target objects. Estimated parameters are continuously transferred to the display side system and the tactile display applies stimuli on the operator.

Tactile sensations occur when mechanoreceptors detect deformation of finger tissue. Factors which cause deformation are kinetic properties such as rubbing speeds or pressing force and physical properties of the objects such as spatial frequencies or Young's modulus. According to the psychophysical studies on roughness sensations, when humans scan the roughness samples like the ones adopted in this study, their subjective sensations are almost determined by groove widths and surface wavelengths of the samples [5][6]. Hence, the present study has selected surface wavelengths as one of the roughness factors.

Fig. 1 is a block diagram of the proposed roughness feeling telepresence system. It is master-slave typed. In the diagram, the tactile sensor estimates surface wavelengths of objects in real-time and transfer them to the display side system. In the display side system, tactile stimuli are generated by combining rubbing speeds and the wavelengths. The system is able to present tactile stimuli in synchronization with touch motions.

III. Real-time Estimation of Surface Wavelengths of Roughness Specimens

A. Tactile Sensor for Estimation of Surface Wavelengths

Tactile sensors for tactile telepresence systems are expected to cause same kinds of physical phenomena such as deformation or stick-slip effect in rubbing objects. This study adopted a tactile sensor emulating the tissue structure and perceptual mechanism of human fingers [7]. Fig. 2 shows a photo and a schematic view of the sensor. The sensor has a layered structure whose layers are designed to have similar

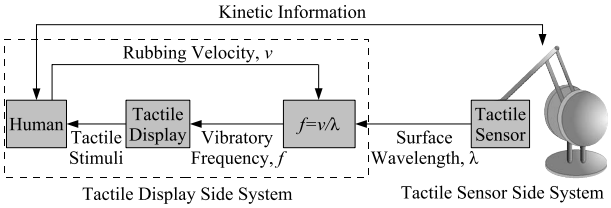

Fig. 1. A block diagram of a master-slave typed roughness feeling telepresence system by surface wavelengths of target objects, which cancels the mismatches between tactile and kinetic sensations of human operators

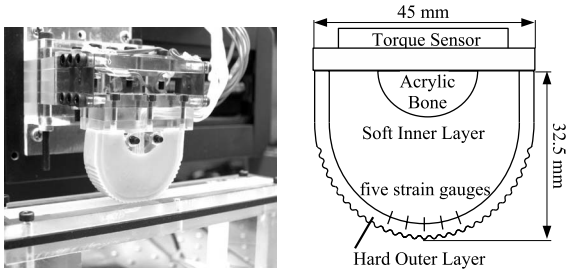

Fig. 2. Tactile sensor adopted in the present study, mimicking the major features of human fingers

Young's moduli of cutaneous fat and epidermis of human fingers. It is covered with ridges which have epidermal ridges like curvatures, and dimensions of the sensor are three times as big as a human finger. Five strain gauges are embedded inside and the sensor is able to acquire vibratory information. A six axial torque sensor is installed on the base of the sensor.

It was confirmed that the sensor could estimate surface wavelengths of objects by computing Fourier transform when it scanned objects at constant speeds, although the computational process was off-line [7]. In the present study, the real-time estimation method has been proposed. This sensor was redundant for the aim of this study. However it can be potentially used for multimodal tactile telepresence system.

B. Algorithm to Estimate Surface Wavelengths in Real-time

The algorithm to estimate surface wavelengths of objects in real-time is described in this subsection. The algorithm estimates a vibratory frequency of the sensor. A surface wavelength can be derived from the relationship of $\lambda = v/f$, where v is a rubbing speed. A frequency element whose spectrum is largest can be considered most influential in perceived roughness while many frequency elements exist in a vibration of the sensor. Therefore, the algorithm was designed to be capable of estimating a major vibratory frequency in real-time.

The sensor scans a roughness sample illustrated in Fig. 3, which is a trapezoidal grating scale whose ridge width and groove width are equivalent. Then band-pass filtered signals of sensory outputs are like in Fig. 4. The pass band of the filter is 5–100 Hz, considering a frequency response of Meissner's corpuscles. The algorithm emits an impulse when the filtered signal crosses a zero level. Fig. 4 shows the example of impulses emitted at zero crosses of sensory outputs. The existence of the impulse is written by (1). The algorithm estimates the vibratory frequency of the sensor by counting the number of the impulses for a certain period A. The estimated vibratory frequency is denoted by (2).

$$p(t) = \begin{cases} 1 & \text{when the impulse is emitted} \\ 0 & \text{when no impulse is emitted} \end{cases} \quad (1)$$

$$f_e(t) = \frac{\Sigma_{\tau=t-A}^{t}\, p(\tau)}{2A} \quad (2)$$

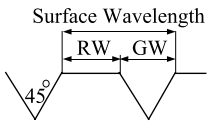

Fig. 3. Acrylic roughness specimen

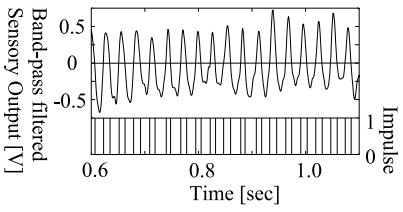

Fig. 4. Example of band-pass filterred sensory outputs and impulses which are emitted at zero crosses

C. Optimization and Numerical Analysis of the Proposed Algorithm

To evaluate the algorithm proposed in the prior subsection and decide an optimal value of A, the algorithm and its expected error are formulated in this subsection. The algorithm estimates a vibratory frequency at t by smoothing the frequency of the past A second. Therefore an estimated vibratory frequency $f_e(t)$ is approximated to be (3).

$$f_e(t) = \frac{\int_{t-A}^{t} f(\tau)d\tau}{A} \quad (3)$$

$$f(t) = \frac{|v(t)|}{\lambda} \quad (4)$$

where $f(t)$ is a true value of a vibratory frequency of the tactile sensor and it is presented by (4). λ is a surface wavelength of the target object and $v(t)$ is a rubbing velocity. The estimated wavelength (5) is derived from (3), (4) and the relationship $\lambda = v/f$.

$$\lambda_e(t) = \frac{|v(t-\frac{A}{2})|}{f_e(t)} + X \quad (5)$$

where X is an error caused by the noise in sensory outputs. The integral computation delays $f_e(t)$ a half A so that $\lambda_e(t)$ refers to $v(t-A/2)$. From above definition (5), the estimated error of the surface wavelength is defined as (6).

$$|\lambda_e(t) - \lambda| = |\frac{|v(t-\frac{A}{2})|}{f_e(t)} - \lambda + X| \quad (6)$$

The optimal A is a value which minimizes (6). A has been designed so that (6) is extremum when $v(t)$ is sinusoidal, which is close to a natural rubbing motion of humans. $v(t)$ is described as (7).

$$v(t) = \alpha \sin(2\pi f_v t) \quad (7)$$

where α is a maximal speed and f_v is a reciprocating frequency of the rubbing motions. With the sinusoidal rubbing velocity, the estimated vibratory frequency is (8) from (3), (4) and (7).

$$f_e(t) = \begin{cases} \frac{\alpha}{Af_v\lambda\pi}|S(\pi f_v A)S(2\pi f_v(t-\frac{A}{2})| \\ \qquad \text{if } t \in T_1 \\ \frac{\alpha}{Af_v\lambda\pi}(1 - |C(\pi f_v A)C(2\pi f_v(t-\frac{A}{2}))|) \\ \qquad \text{if } t \in T_2 \end{cases} \quad (8)$$

$$S(x) = sin(x), C(x) = cos(x)$$
$$\forall t(t \in T_1 \leftrightarrow v(t)v(t-A) \geq 0)$$
$$\forall t(t \in T_2 \leftrightarrow v(t)v(t-A) < 0)$$

As a visual aid of (8)! $v(t), f(t-A/2), f_e(t)$ and $\lambda_e(t)$ are plotted in Fig. 5.

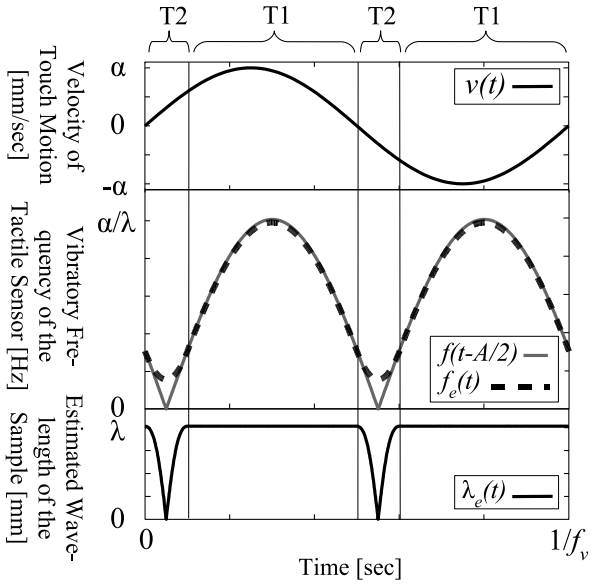

Fig. 5. Examples of simulated values of the rubbing velocity $v(t)$, the true and the estimated vibratory frequencies $f(t-A/2), f_e(t)$ and the estimated wavelength $\lambda_e(t)$: $A = 0.2$ sec, $\lambda = 2.0$ mm, $\alpha = 100.0$ mm/sec, $f_v = 1.0$ Hz, $X = 0$ mm

Fig. 5 implies that accuracy of estimation is deteriorated in range T_2, in which acceleration of velocity is larger than range T_1 or the direction of velocity is about to change. In the algorithm, the mean value for a period becomes an estimated vibratory frequency; therefore it makes sense that precision is deteriorated when the rubbing motion is highly accelerated or decelerated. Also, the algorithm is designed to perform when the sensor is completely slipping on objects. However, the sensor and the objects are considered to stick when a relative velocity between them is slow. Therefore, different algorithms should be applied to range T_1 and T_2 for estimation.

The proposed algorithm is suitable for range T_1. For further evaluation of range T_1, the estimated error of surface wavelength (9) is derived from (6), (7) and (8).

$$\begin{aligned} |\lambda_e(t) - \lambda| &= |\frac{Af_v\lambda\pi}{\sin(Af_v\pi)} - \lambda + X| \\ &\leq \lambda|\frac{Af_v\pi}{\sin(Af_v\pi)} - 1| + |X| \end{aligned} \quad (9)$$

where the estimated error of surface wavelengths is the sum of the approximation error (1st term) and the error caused by signal noise (2nd term). Assuming that noise is subject to normal distribution, $N(0, \sigma^2)$, the expected value of $|X|$ is denoted as (10).

$$E(|X|) = \frac{2\sigma}{\sqrt{2\pi A f_s}} \quad (10)$$

where f_s is a sampling frequency. According to (10), as the sampling period A rises, the increased number of samplings for the computation reduces the effect of noise.

The estimated error of the surface wavelength is redefined as (11) from (9) and (10).

$$|\lambda_e(t) - \lambda| = \lambda|\frac{Af_v\pi}{\sin(Af_v\pi)} - 1| + \frac{2\sigma}{\sqrt{2\pi Af_s}} \qquad (11)$$

In (11), the condition to make the approximation error zero is $Af_v \to 0$. However, the smaller A is, the larger the effect of noise becomes. Both the approximation error and the error caused by noise must be balanced. The optimal value of A is decided so that (11) reaches its minimum value.

It is fair to guess that A is not a fixed value and should be adaptive to environments, referring some variables. Equation (11) implies that A should be adjusted according to f_v, which is the reciprocating frequency of the rubbing motions. Because in (11), A always appears with f_v in the first term. However, it is not straightforward to estimate f_v in real-time. The authors assigned 1 Hz to f_v as a representative value since the reciprocating frequency of natural touch motions is supposed 0–2 Hz. A standard deviation σ was assigned 1.0 mm, which was from a standard deviation of the estimated values when the sensor actually scanned the roughness sample whose wavelength was 1 mm at 70 mm/sec. f_s was 1 kHz. Under the above conditions, A was determined to be 0.080 seconds.

D. Experimental Evaluation

Four roughness samples used in experimental evaluation were depicted in Fig. 3. Their wavelengths were 1–4 mm with an interval of 1 mm. In the experiment, the sensor was installed on a vertical slider which was fixed on a single-axis arm. The sensor was pressed to the samples with a depth of 1 mm in a static state (the reaction force was about 0.6 N), then it scanned samples. The photo of the experimental setup is Fig. 10.

1) Evaluation of Precision: Precision of estimation was measured when the sensor scanned the samples at constant speeds which varied from 30 to 70 mm/sec. The mean values of the estimated surface wavelengths were computed from data which were recorded for two seconds. Those computed values are shown in table I. Table I shows that four wavelengths were completely discriminated. Fig. 6 is a graph of table I. To equally dispose dots along the temporal axis, seven more experimental results were added to table I. In Fig. 6, the horizontal axis is the vibratory frequency defined by v/λ. The vertical axis is accuracy of estimation, which is a ratio of the estimated and the true values of the surface wavelengths. Fig. 6 suggested that accuracy of estimation depended on the vibratory frequency of the sensor and the rubbing speeds. The sampling period of the algorithm was 0.08 seconds; hence accuracy was not good with the vibratory frequency less than about 10 Hz. The frequency of stick-slip phenomena was quick enough that the band-pass filter could not eliminate its effect when rubbing speeds were fast. Therefore, the accuracy was not good with high vibratory frequencies in Fig. 6.

TABLE I

MEAN VALUES OF ESTIMATED SURFACE WAVELENGTHS WHEN SAMPLES WERE SCANNED AT CONSTANT SPEEDS

Rubbing speed, v [mm/s]	Wavelengths of Samples, λ [mm]			
	1.0	2.0	3.0	4.0
30	1.006	2.072	3.390	4.321
50	1.006	1.844	3.096	4.038
70	1.128	1.978	3.023	4.075

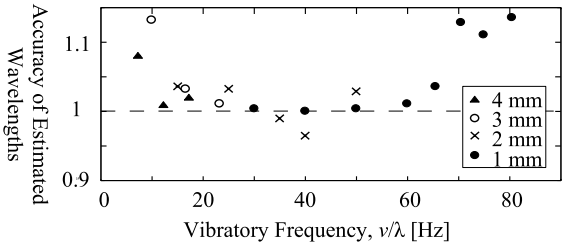

Fig. 6. Accuracy of wavelength estimation when samples were scanned at constant speeds

2) Evaluation at the Sinusoidal Velocity: An example of the transition of the estimated wavelength when the sensor scanned the sample at the sinusoidal velocity is shown in Fig. 7. The wavelength of the sample was 2 mm. For the most part, the wavelength was estimated well. However in contrary to the numerical analysis in III-C and Fig. 5, even in range T_1 accuracy was deteriorated. The same trend was observed at other speeds and the reciprocating frequencies. It is considered that this performance decline was caused by the unexpectedly shorter slipping phases, and the algorithm was designed to perform on the assumption that the sensor slipped on objects. This problem can be solved by introducing detection of slipping phases.

3) Evaluation of Real-time Property: The experiment for evaluating the real-time property of the algorithm was conducted. From a nature of the algorithm, the estimated value is computed from sensed data for the past 80 milliseconds, the algorithm can deal with a sudden change of wavelengths in 80 milliseconds. Fig. 8 shows the transitions of the sensory

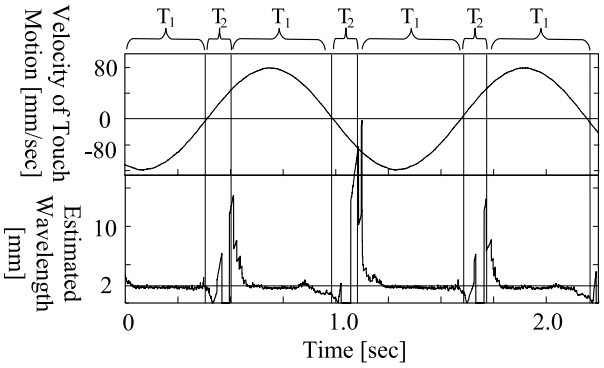

Fig. 7. A transition of the estimated surface wavelength when the sensor scanned the sample at the sinusoidal velocity; $\lambda = 2$ mm, $v = 70\sin(2\pi 0.83t)$ mm/sec

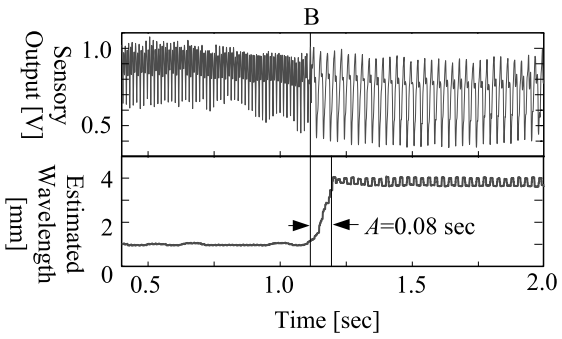

Fig. 8. Example of the sensory outputs and the estimated surface wavelengths when the sensor scanned two different specimens

outputs and the estimated wavelengths when the sensor scanned two roughness samples, which were arranged side by side beneath the sensor. The wavelengths of the samples were 1 mm and 4 mm. At point B in Fig. 8, the sensor reached the boundary of two samples, then 80 milliseconds later the estimated value was roaming around 4 mm.

From above three kinds of evaluation, the algorithm has potential to transfer differences of surface wavelengths from 1 to 4 mm by 1 mm in real-time.

IV. Roughness Display Method Via ICPF Tactile Display

The present study employed ICPF tactile display [8]. Fig. 9 shows pictures of the display. The device is light, wearable and does not constrain touch motions of the operator. It composes of fifty pieces of gel actuators made of ionic conductive polymer films, which bend when electric voltages are applied. The actuators respond to high frequencies more than 200 Hz. Desired tactile stimuli are generated by controlling vibration of the actuators. The voltages for the actuators were given by (12).

$$y = 5.0 \sin\left(2\pi \frac{v}{\lambda} t\right) \ [V] \tag{12}$$

where v was a speed of the hand movement and λ was the surface wavelength of the samples. The maximal voltage effects on generating force by the actuators. Waveforms and generating force were not considered in (12). Only the vibratory frequencies of the stimuly was controlled in response to hand motions.

Resolution of displayable wavelengths by the method was investigated by a psychophysical experiment. In the test, each

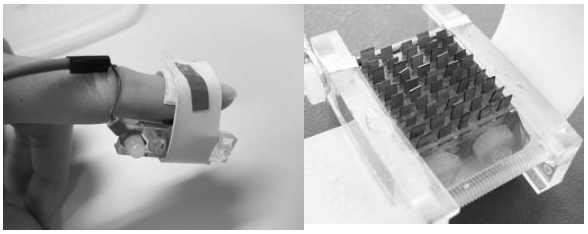

Fig. 9. Tactile display adopted in the present study

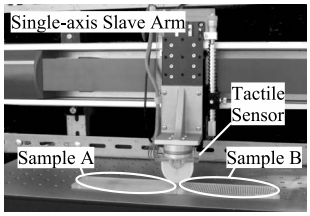

Fig. 10. Slave side system

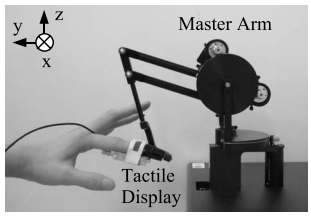

Fig. 11. Master side system

TABLE II
SPATIAL WAVELENGTH DISCRIMINATION LIMENS MEASURED BY LIMITATION METHOD WHEN THE STIMULI WERE GIVEN BY ICPF TACTILE DISPLAY (AVERAGE OF THREE SUBJECTS)

	Standard stimuli [mm]			
	1.0	2.0	3.0	4.0
Average lower limen	0.82	1.78	2.80	3.55
Average upper limen	1.28	2.14	3.42	4.40
Avg. discrimination limen	0.23	0.18	0.31	0.43
SD of discrimination limen	0.095	0.10	0.082	0.13

subject equipped his index finger with ICPF tactile display and stuck it through a tip of a master arm. The appearance of the test looked like Fig. 11. The subject moved his hand along x-axis and v was an x directional element of the velocity. To constrain the hand movements on the x-y plane, a virtual plane was made by the master arm.

Wavelength discrimination limens were measured by limitation method. Standard stimuli were 1, 2, 3, 4 mm and comparison stimuli were given by 0.2 mm. Two ascending series and two descending series were given per a standard stimulus. The subject could orally switch the standard and the comparison stimulus. There was no time limit in the tests. He answered which surface wavelength he felt longer. The answers were manually recorded by an experimenter. The subjects were three men in their twenties. The measured discrimination limens are shown in table II. Table II shows that the discrimination limens were smaller than 1 mm and it is concluded that the display method has an ability to display differences in wavelengths by 1 mm.

V. Roughness Feeling Telepresence System

In this section, the roughness feeling telepresence system which combines the tactile sensor and the display is described. It was confirmed that the sensor and the display could discriminate the wavelengths by 1 mm individually in prior sections. The integrated performance and results of the experiment to transfer surface wavelengths are shown.

A. System Integration

In the integrated system, the tactile sensor was installed on a single axis arm as shown in Fig. 10 and it was controlled to move at the velocity same as the x-directional velocity of the master arm. The tactile display was equipped an index finger of a subject like Fig. 11. The sensor continuously estimated the wavelengths of the samples and the estimated values were transferred to the display side system at 100 Hz. Among the

TABLE III

EXPERIMENTAL RESULTS OF WAVLENGTH TRANSFER: PERCENTAGES OF CORRECT ANSWERS

	4 mm	3 mm	2 mm	1 mm
4 mm	-	0.7	1.0^{***}	0.9^{*}
3 mm	-	-	0.9^{*}	0.7
2 mm	-	-	-	0.9^{*}

*** and * are significant at level 99.9% and 95% respectively.

TABLE IV

THURSTONE CASE V SCALES OF TRANSMITTED WAVELENGTHS

Sample	1 mm	2 mm	3 mm	4 mm
Score	0	0.5461	1.092	1.449

all estimated values, values in range T_1 were used. Based on the transferred wavelengths and the rubbing velocity of the subject, applied voltages were determined by (12) for the tactile stimuli.

B. Experimental Methodology

Four roughness samples whose wavelengths were 1–4 mm were used in the experiment. The number of the subjects was one and he was one of the three subjects tested in section IV. He was considered to have an ability to discriminate the four samples. The experimental method was paired comparison. Six combinations were made from the four samples and each pair was tested ten times. The systems were disposed so that the subject could not see the tactile sensor side system. He knew that two different specimens were arranged at the right and the left side of the initial position of his hand. He was allowed to freely check two samples and answered which sample had a longer wavelength.

C. Experimental Results

Table III shows the experimental results. A value in a cell is a percentage of the correct answers, when the subject tested two samples whose wavelengths were designated by a row and a column. Z-test with no consideration of multiplicity showed that four among six pairs were significantly discriminated. Table IV shows Thurstone Case V scores computed from table III. Internal consistency of the model was tested by Mosteller's χ^2 test and the model fit the experimental case ($\chi^2 = 8.72$ and $\chi^2 < \chi^2_7(0.05) = 14.07$).

VI. DISCUSSION AND FUTURE WORKS

In the experimental results, as to two pairs, the subject could not discriminate two samples in a view of statistics. To improve the abilities of the telepresence system, the sensor and the display system should be individually sophisticated. Detection of the slipping phases of the tactile sensor contributes to accuracy of wavelength estimation because the algorithm used in this study did not perform in those phases. It is necessary for the display method to involve physical parameters other than spatial wavelengths, although this study simply controlled unique temporal frequencies of the actuators.

The metric for the tactile telepresence systems is needed, considering perceptual characteristics of humans. The abilities of the systems cannot be simply compared with the case that bear fingers scan objects. All actuators in the employed tactile display were driven in the same phase, and they did not cause spatial distribution in the contact area between a finger. Under the similar condition, roughness sensations are impaired [9][10].

VII. CONCLUSION

The present study has proposed a new framework of tactile telepresence systems, which is suitable for remote environments. In the proposed framework, in order to cancel latency between kinetic and tactile sensations, tactile stimuli are generated by combining physical parameters of target objects and touch motions of operators in a local loop of the display side system. A roughness feeling telepresence system was implemented based on the framework and it was confirmed that a subject could discriminate a physical character of roughness specimens through the system.

REFERENCES

[1] R. D. Howe, W. J. Peine, D. A. Kontarinis and J. S. Son, Remote Palpation Technology, IEEE Engineering in Medicine and Biology, Vol. 14, Issue 3, pp. 318–323, 1995

[2] Maria Vatshaug Ottermo, Oyvind Stavdahl, Tor A. Johansen, Palpation Instrument for Augmented Minimally Invasive Surgery, Proceedings of the 2004 IEEE/RSJ International Conference on Intelligent Robots and Systems, pp. 3960–3964, 2004.

[3] Antonio Bicchi, Enzo P. Schilingo and Danilo De Rossi, Haptic Discrimination of Softness in Teleoperation: The Role of the Contact Area Spread Rate, IEEE Transactions on Robotics And Automation, Vol.16, Issue 5, pp. 305–310, 2000

[4] Akio Yamamoto, Shuichi Nagasawa, Hiroaki Yamamoto, and Toshiro Higuchi, Electrostatic Tactile Display with Thin Film Slider and Its Application to Tactile Tele-Presentation Systems, IEEE Transactions on Visualization & Computer Graphics, Vol. 12, No. 2, pp. 168–177, 2006

[5] Takashi Yoshioka, Barbara Gibb, Andrew K. Dorsch, Steven S. Hsiao and Kenneth O. Johnson, Neural Coding Mechanisms Underlying Perceived Roughness of Finely Textured Surfaces, The Journal of Neuroscience, Vol. 21, pp. 6905–6916, 2001

[6] Carissa J. Cascio and K. Sathian, Temporal Cues Contribute to Tactile Perception of Roughness, The Journal of Neuroscience, Vol. 21, pp. 5289–5296, 2001

[7] Y. Mukaibo, H. Shirado, M. Konyo and T. Maeno, Development of a Texture Sensor Emulating the Tissue Structure and Perceptual Mechanism of Human Fingers, Proceedings of the 2005 IEEE International Conference on Robotics and Automation, pp. 2565–2570, 2005

[8] Masashi Konyo, Satoshi Tadokoro, Toshi Takamori, Keisuke Oguro, Artificial Tactile Feel Display Using Soft Gel Actuators, Proceedings of the 2000 IEEE International Conference on Robotics and Automation, pp. 3416-3421, 2000

[9] Roberta L. Klatzky and Susan J. Lederman, Tactile roughness perception with a rigid link interposed between skin and surface, Perception & Psychophysics, Vol. 61, Issue 4, pp. 591–607, 1999

[10] Efrat Gamzu and Ehud Ahissar, Importance of Temporal Cues for Tactile Spatial-Frequency Discrimination, The Journal of Neuroscience, Vol. 21, pp. 7416–7427, 2001